JOURNAL OF BONE AND MINERAL RESEARCH
Volume 16, Number 4, 2001

Low-Intensity Pulsed Ultrasound Accelerates Rat Femoral Fracture Healing by Acting on the Various Cellular Reactions in the Fracture Callus

YOSHIAKI AZUMA,[1] MASAYA ITO,[1] YOSHIFUMI HARADA,[1] HIDEKO TAKAGI,[1] TOMOHIRO OHTA,[1] and SEIYA JINGUSHI[2]

ABSTRACT

Low-intensity pulsed ultrasound (LIPUS) has been shown to accelerate fracture healing in both animal models and clinical trials, but the mechanism of action remains unclear. In fracture healing, various consecutive cellular reactions occurred until repair. We investigated whether the advanced effects of LIPUS depended on the duration and timing of LIPUS treatment in a rat closed femoral fracture model to determine the target of LIPUS in the healing process. Sixty-nine Long-Evans male rats that have bilateral closed femoral fractures were used. The right femur was exposed to LIPUS (30 mW/cm^2 spatial and temporal average [SATA], for 20 minutes/day), and the left femur was used as a control. Rats were divided into four groups according to timing and duration of treatment (Ph-1, days 1–8; Ph-2, days 9–16; Ph-3, days 17–24; throughout [T], days 1–24 after the fracture). Animals were killed on day 25. After radiographs and microfocus X-ray computed tomography (μCT) tomograms were taken, the hard callus area (HCA), bone mineral content (BMC) at the fracture site, and mechanical torsion properties were measured, and histological analysis was conducted. Interestingly, the maximum torque of the LIPUS-treated femur was significantly greater than that of the controls in all groups without any changes in HCA and BMC. The multiviewing of three-dimensional (3D) μCT reconstructions and histology supported our findings that the partial LIPUS treatment time was able to accelerate healing, but longer treatment was more effective. These results suggest that LIPUS acts on some cellular reactions involved in each phase of the healing process such as inflammatory reaction, angiogenesis, chondrogenesis, intramembranous ossification, endochondral ossification, and bone remodeling. (J Bone Miner Res 2001;16:671–680)

Key words: **low-intensity pulsed ultrasound, fracture healing, fracture callus, mechanical properties, mechanical stress**

INTRODUCTION

ULTRASOUND IS used widely in surgery, therapeutics, and diagnostics.[1] The frequency used ranges from 0.8 to 15.0 MHz, which is based on considerations of sound absorption, penetration, and resolution. The intensities are high for surgical and therapeutic applications (1–50 W/cm^2) and are designed to cause significant tissue heating.[2] Diagnostic ultrasound employs much lower intensities (1–50 mW/cm^2), which are chosen specifically to avoid tissue heating.[1]

Fracture healing has been accelerated by exposure to a specific pulse of extremely low-intensity pulsed ultrasound (LIPUS) in the latter power range in both animal fracture models and clinical trials.[3–9] For example, Heckman et al. reported that LIPUS treatment for 20 minutes/day at 30

[1]Teijin Institute for Biomedical Research, Teijin Limited, Tokyo, Japan.
[2]Department of Orthopedic Surgery, Graduate School of Medical Science, Kyushu University, Fukuoka, Japan.

mW/cm^2 led to a significant 24% reduction in the time required for clinical healing in a prospective randomized placebo-controlled study of closed or grade I open tibial fractures.[8] Additionally, Kristiansen et al. showed that the time until union was 38% shorter for patients treated with LIPUS than for those treated with placebo in a multicenter prospective randomized placebo-controlled clinical trial of dorsally angulated fractures of the distal radius.[9] However, the physical process through which LIPUS stimulates living tissue remains unclear. LIPUS is a form of mechanical energy that can be transmitted into living tissue as high-frequency acoustical pressure waves. The micromechanical strains produced by these pressure waves in living tissue can result in biochemical events at the cellular level.[10–12] Duarte indicated that a pulsed ultrasound intensity of 49.6 mW/cm^2 and 57 mW/cm^2 spatial average and temporal average (SATA) was nonthermal.[4] In this experiment, we used LIPUS (30 mW/cm^2), which is considered to have little thermal effect and to produce stable cavitation and streaming. Wang et al. reported a technique for exposing standard closed femoral fractures to LIPUS and confirmed that LIPUS stimulation enhanced the mechanical properties of the healing callus.[7] Their observations imply that cells in the fracture callus sense and respond to the mechanical energy transferred by the LIPUS.

Fracture healing occurs in a stepwise process of various cellular reactions until the fracture has been repaired.[13] Cell types, such as endothelial cells, fibroblasts, osteoblasts, chondrocytes, and osteocytes, all of which respond to mechanical stress or mechanical strain,[14–18] play important roles in the fracture healing process.[19] The mechanical energy transferred by LIPUS therefore might act on various processes such as inflammatory reaction, angiogenesis, chondrogenesis, intramembranous ossification, endochondral ossification, or bone remodeling in the fracture callus.

In previous experiments using a rat closed femoral fracture model, we found accelerating effects of daily LIPUS treatment until 21 days after the fracture (in preparation). Because in this model a series of stage-specific cellular reactions were observed until repair,[20] we investigated whether the advanced effects of LIPUS depended on duration and timing of LIPUS treatment in this model to determine the target reaction of LIPUS in the fracture healing process in vivo. In the present study, we divided the interval up to 25 days after the fracture into three periods (Ph-1, Ph-2, and Ph-3), each of which involved different essential reactions for fracture healing,[20] and investigated the effects of partial treatment with LIPUS on the fracture healing. If the advanced effects of LIPUS on fracture healing are based on an effect on a specific reaction, the efficiency of acceleration should depend on the timing of the partial LIPUS treatment. In this study, we investigated the relationship between the timing of the partial LIPUS treatment and the efficiency of accelerating action by estimating mechanical properties, bone mass, histology, and the microstructure of the callus, the latter by using the three-dimensional (3D) microfocus X-ray computed tomography (μCT) technique.

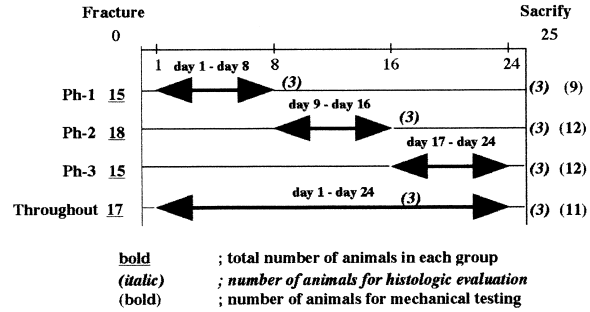

FIG. 1. Experimental schedule for LIPUS treatment regimens. The animals in each group were treated with LIPUS as follows: the duration was in the Ph-1 group from day 1 to 8 after the fracture (8 days), in the Ph-2 group from day 9 to 16 after the fracture (8 days), in the Ph-3 group from day 17 to 24 after the fracture (8 days), and in the T group from day 1 to 24 after the fracture (24 days). All remaining animals were killed on day 25 after the fracture.

MATERIALS AND METHODS

Closed femoral fracture model

A total of 69 skeletally mature 10-week-old male Long-Evans rats (Charles-River Laboratories, Inc., Wilmington, MA, USA), weighing 300–350 g, were used for this study. All rats were housed at 24 $\pm$ 2°C, a relative humidity of 55 $\pm$ 10% with a 12-h/12-h light/dark cycle. The rats were fed standard rat chow (CE2) obtained from Clea Japan, Inc. (Tokyo, Japan) and were given water ad libitum. The closed femoral fracture models were produced by the method previously described.[21] Under anesthesia induced by intraperitoneal (ip) injection with sodium pentobarbital (50 mg/kg per ml; Dinabot, Inc., Osaka, Japan), a medial parapatellar arthrotomy was made, and the patella was then dislocated laterally. The medullary canal was entered through the intercondylar notch and reamed with a 19G needle. A 1 mm $\times$ 28 mm Kirschner wire (Natsume Co., Ltd., Tokyo, Japan) was then inserted into the canal. The patella was relocated, and then the soft tissues were closed with no. 4.0 silk sutures. The stabilized femur was placed in a three-point bending device (Arizono Machine Co., Ltd., Kagoshima, Japan), and the femur was fractured by the force of a 500-g weight dropped from a height of 35 cm. Bilateral fractures were made in all animals. Radiographs were used to confirm of the position and orientation of each fracture. Because we used rats that satisfied the inclusion criteria only, the sample size in each group was unequal. Three rats in the Ph-1 group and one in the throughout (T) group did not satisfy the criteria. Because those rats were not used for LIPUS treatment, a total of 65 animals were used as shown in Fig. 1. Our Institutional Animal Care and Use Committee approved all procedures.

LIPUS signals

The LIPUS exposure system used, which was a modification of the device used in experiments by Wang et al.,[7] was made by Medical Engineering Research Laboratories of

Teijin, Ltd. (Tokyo, Japan). It consisted of a function generator (model HP33120A; Hewlett-Packard Japan, Ltd., Tokyo, Japan), a power supply, and six lead-zirconate titanate transducers (PZT-4, effective area of 3.88 cm^2). With it, six animals could be exposed to LIPUS at the same time. The LIPUS signal was generated with a transducer and was composed of a 200-μs burst sine wave of 1.5 MHz repeating at a frequency of 1.0 kHz. The 200-μs burst of pressure pulses was followed by an off time of 800 μs and was repeated every millisecond. The LIPUS intensity was 30 mW/cm^2 as an SATA. The LIPUS signal and times per day used in this study were the same as those recommended for a clinical device (Sonic Accelerated Fracture Healing System [SAFHS; Exogen, Inc., Piscataway, NJ, USA]). The LIPUS signal conditions were calibrated with a hydrophone system that consisted of an oscilloscope (model OS-111; Hewlett-Packard Japan, Ltd.) and a PZT-4 transducer for detection. The LIPUS intensity was calibrated with an ultrasound power meter (model 101; OR Instruments, Inc., Seattle, WA, USA) before LIPUS exposure to the animals. The interexperiment CVs of each transducer was within 10% for the LIPUS intensity.

Duration and timing of LIPUS treatment

The animals were treated with LIPUS while they were under ip anesthesia with ketamine (20–60 mg/kg) and xylazine (2.5 mg/kg). The anesthetized rats were placed on their back on the holder. Ultrasound gel (Nippon Kohden Co., Ltd., Tokyo, Japan) was applied to the shaved fracture area in the medial aspects of both thighs of all animals. The transducer was placed close to the skin covered with ultrasound gel at the femoral fracture site. The animals were exposed to LIPUS once daily for 20 minutes. The right femur of the rats was exposed to the LIPUS transducer, and the left femur was used as the nontreated contralateral control. The duration and timings of the LIPUS treatment are shown in Fig. 1. The animals in each group were treated with LIPUS as follows: LIPUS treatments were performed in the Ph-1 group for 8 days, from day 1 to 8 after fracture; in the Ph-2 group for 8 days, from day 9 to 16 after fracture; in the Ph-3 group for 8 days, from day 17 to 24 after fracture; and in the T group for 24 days, from day 1 to 24 after fracture. Animals were killed on day 25 after the fracture.

Radiography and bone mineral content at the fracture site

The femora were collected on day 25 after the fracture. All femora were radiographed with a soft X-ray system (model CSM; Softex Co., Ltd., Tokyo, Japan). After the soft tissues had been dissected from the femora, the intramedullary pins were removed. Bone mineral content (BMC) in the area near the fracture site was measured with a dual-energy X-ray absorptiometer (DXA; model QDR-2000; Hologic, Inc., Waltham, MA, USA). The scan field size was 3.48 $cm^2 \times 1.41$ cm^2, and the resolution was 0.0254×0.0127 cm^2. The area near the fracture site of each femur was determined as the area extending 3.6 mm on either side of the fracture line, which was measured with software for high-resolution analysis. The CV for the measurement of the BMC of standard samples by this technique was 0.8%. Specimens were stored in saline-soaked gauze at −20°C.

Hard callus area

Radiographic signals of each femur and the standard scale were captured as digitized images with a scanner and stored on a Macintosh computer using Adobe PhotoShop version 4 software. The area of the outer hard callus was measured by tracing the callus portion with "National Institutes of Health (NIH) image version 1.6" image analysis software (NIH, Bethesda, MD, USA). The area represents the number of pixels within each tracing. The standard scale also was measured, and the pixel value of each hard callus area (HCA) was transferred to the value of the real scale.

Mechanical testing

Just before mechanical testing, the specimens were thawed at room temperature for 2 h. Both bone ends were embedded in polyacrylic resins (GC-OSTORON; GC Dental Products Co., Ltd., Aichi, Japan). A custom-made jig ensured consistent alignment of the bone axis with the axis of the testing machine. All specimens were tested to failure in torsion at room temperature on an electromechanical testing machine (model MZ-500D; Maruto Machine, Inc., Tokyo, Japan) at the rate of 1.5°/s with 111.5 g of weight as axial load. Maximal torque until failure and torsional stiffness (the tangent at the point of maximal slope) were calculated from the load-deformation curve. The biomechanical stages of fracture union were determined based on pattern of failure according to White et al.[22]

Histological evaluation

Three rats per each group were killed, and the femora were collected on day 25 after the fracture for histological evaluation. To observe the effect of LIPUS in progress on day 9 and day 17 after fracture, we killed three rats in the Ph-1 and Ph-2 groups, respectively. The femora were fixed for several days in 10% neutral buffered formalin. After the μCT images had been obtained, the femora were treated with 10% formic acid for 1 h, transiently. Then, the femora were decalcified with 10% EDTA solution and embedded in paraffin. Three to five sections (6 μm thick) were cut through the long axis of each femur in the sagittal plane and stained with Masson's trichrome stain and hematoxylin and eosin stain. The section that had the maximum diameter was chosen as the representative section for each fracture.

3D μCT analysis

The μCT (model NX-CP-C80H-IL) equipment that produced the tomograms had been especially developed by Nittetsu ELEX Co., Ltd. (Osaka, Japan). The device has a maximum experimental spatial resolution of 2.5 μm and a minimum slice thickness of 5 μm for measurements of a ceramic standard sample. The fan beam of μCT has a small

focal spot size, 3 μm in diameter, a conventional microfocus open vacuum-type X-ray source, rotating sample stage, 1024 linear response image sensors, and image intensifier (image sensors). A total of 100 cross-sectional tomograms per femur were obtained with a slice thickness of 80 μm and reconstructed at 512 $\times$ 512 pixels, by use of an acceleration voltage of 30 kV and current of 0.1 mA. To evaluate the bone bridging at the fracture site by use of a 3D reconstruction technique, we took 50 slices extending (4000 μm) on either side of the fracture line. The 3D reconstruction of 100 tomograms was performed by the volume-rendering method (software, VIP-Station; Teijin System Technology, Inc., Kanagawa, Japan) using a computer (model SUN SPARK-5; Sun Microsystems, Inc., Palo Alto, CA, USA). By use of the computer software, the threshold of each image was kept at the same level to observe trabecular bone and cortex of the healing callus. At this threshold, we never detected the soft callus of the femur. Electronic sections were cut through the long axis of each femur in the sagittal plane on 3D reconstructed images. The home sagittal plane (0°) was identified as that which was used to cut through the long axis of the original 3D reconstructed image of each femur. To estimate the bone bridging in detail, we rotated the sagittal plane clockwise about the long axis at 60° increments of pitch (0°, 60°, 120°, 180°, 240°, and 300°) from the home position in a circuit and cut electronic sections through the long axis of each femur in each sagittal plane.

Statistical analysis

The primary analyses conducted in this study were intraexperimental group comparisons of the treated fractures with the untreated contralateral fractures. Paired *t*-testing was used for analyses of HCA, BMC, and mechanical measurement data. The significance of interexperimental group comparison of mechanical measurement data was determined by a one-way analysis of variance (ANOVA) test. A confidence level of 95% ($p < 0.05$) was chosen for significance.

RESULTS

Mechanical properties of fracture callus

The maximal torque and stiffness in torsion of the fractured femur on the LIPUS-treated side was significantly higher than that of the contralateral control side in all groups (Fig. 2). This indicates that the partial treatment with LIPUS during Ph-1, Ph-2, or Ph-3 also is able to improve the mechanical properties of the fracture callus, as it does with treatment throughout the 24 days. Furthermore, the maximal torque for the LIPUS-treated side in the T group (193 $\pm$ 39 N-mm) was significantly higher than that for the other three groups: Ph-1, 170 $\pm$ 39 N-mm; Ph-2, 159 $\pm$ 31 N-mm; and Ph-3, 161 $\pm$ 34 N-mm (Fig. 2A). The data for stiffness was almost the same as that for maximal torque (Fig. 2B). These results show that the continuous treatment with LIPUS was more effective toward the improvement of the mechanical properties of the fracture callus than the partial treatment.

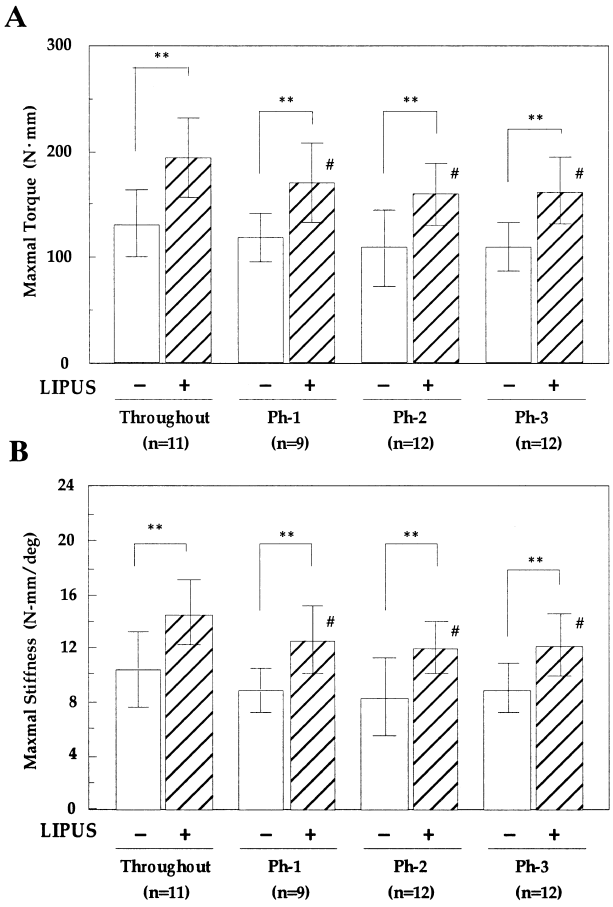

FIG. 2. Effects of LIPUS treatment of various durations and timings on (A) torsional torque and (B) torsional stiffness of fracture callus on day 25 in rat femoral fractures. The torsional torque of LIPUS-treated femurs (closed bars) was significantly higher than that of the nontreated femurs (open bars) in the T group ($n = 11$), Ph-1 group ($n = 9$), Ph-2 group ($n = 12$), and Ph-3 group ($n = 12$). The horizontal bars represent $\pm$ 1 SD. The value of $p < 0.01$ for each treatment group compared with the control side. Paired *t*-testing was used for statistical analysis to compare between the LIPUS-treated side and -nontreated side in each group. The T group showed a significant difference as compared with the partially treated groups. One-way ANOVA was used for statistical analysis to test for significance versus the T group.

Radiographs and 3D μCT analysis

As shown in Fig. 3, in the LIPUS-treated femur, the obliteration of the fracture line at the fracture gap in all groups (Figs. 3B–3E) was more advanced than that in the control femur (Fig. 3A).

The fracture line of the LIPUS-treated femur was bridged by new bone formation 3D in all groups (Fig. 4). In contrast, bridging of the fracture site by new bone formation did not occur substantially in the contralateral LIPUS-untreated control femur. In the LIPUS-treated femur, the bridging of newly formed cortex and trabecular bone in the fracture callus in the T group was greater than that in the Ph-1, Ph-2, and Ph-3 groups. These data show that the beneficial effect of LIPUS treatment on the mechanical properties of fracture

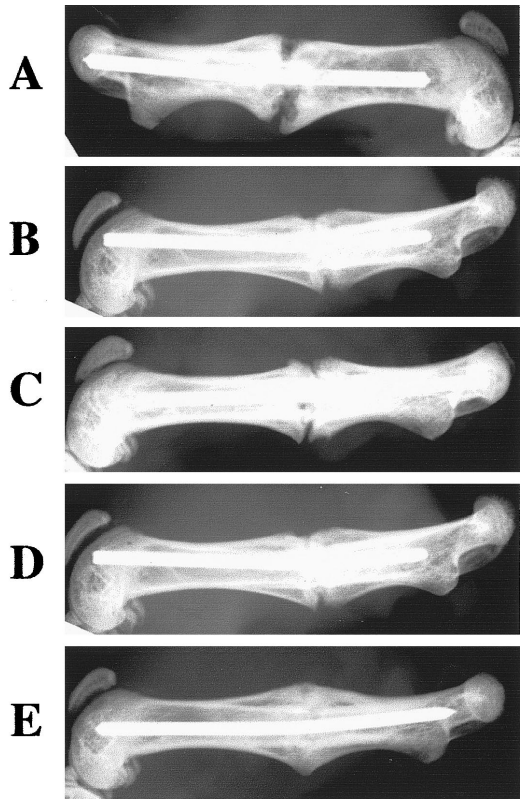

FIG. 3. Radiography of LIPUS-treated femur and nontreated femur in each group at day 25 after the fracture. (A) Nontreated femur and (B–E) LIPUS-treated femur, which are (B) Ph-1, (C) Ph-2, (D) Ph-3, and (E) T, respectively. The femora were collected on day 25. All femora including intramedullary pins were radiographed with a soft X-ray system before dissection of soft tissue.

callus in each group is based on the improvement of the fracture union.

HCA and BMC at fracture site

To determine the effects of LIPUS on the size of the fracture callus, we examined the outer HCA of the fractured femur (Fig. 5A). Mean values of the HCA of femoral fracture callus were approximately 20 mm^2 in all groups on day 25 after the fracture (Fig. 6). There was no significant difference in the HCA between LIPUS-treated femurs and contralateral control femurs in any of the groups (Fig. 6).

Because LIPUS did not affect the size of callus by 25 days after the fracture, we measured BMC at the fracture site to determine the bone mass in the callus (Fig. 5B). Values for BMC at the femoral fracture site on day 25 after the fracture are shown in Fig. 7. Mean values of the BMC in all groups were equivalent and approximately 0.028 g/area on day 25. There were no significant differences in BMC between the LIPUS-treated side and the contralateral control side of the femoral fracture site in any of the groups. These data suggest that the beneficial effect of LIPUS treatment on the mechanical properties of the fracture callus in each group was independent of the size and bone mass of the callus.

Histological evaluation

To examine the effects of LIPUS treatment on fracture healing of the rat femur at the tissue and/or cellular level, we used three rats per group (various durations and timings of LIPUS treatment) for the histological evaluation. This histological evaluation was a qualitative assessment. Histology of LIPUS-treated femurs in the T group on days 9, 17, and 25, and in the Ph-2 and Ph-3 groups on day 17 and day 25 after the fracture are shown in Figs. 8–10.

Early endochondral ossification on day 9 in the LIPUS-treated femur (Fig. 8B) was greater than that in the control (Fig. 8A). In this case, mature cartilage tissue was observed on both the control side and the LIPUS-treated side, but the numbers of the hypertrophic chondrocytes and chondroclasts near the boundary between the cartilage tissue and trabecular bone were greater in the LIPUS-treated side than in the control side. These results suggest that LIPUS treatment in the earlier period (Ph-1) give more advanced cartilage formation and early endochondral ossification in the LIPUS-treated femur than in the control on day 9 after fracture.

On day 17, endochondral ossification in the LIPUS-treated femur (Figs. 9B and 9C) tended to be higher than that in the control (Fig. 9A). The LIPUS-treated femur in the Ph-2 group (Fig. 9B) on day 17 had received LIPUS treatment from day 9 to 16 (for 8 days), and that in the T group (Fig. 9C) on day 17 from day 1 to 16 (for 16 days) after the fracture. Early remodeling of trabecular bone in the hard callus also was observed in all femurs. However, the size of the mature cartilage in the LIPUS-treated femur was smaller than that in the control femur. The number of osteoclasts on the trabecular bone surface in the hard callus also was higher in the LIPUS-treated femur than that in the control.

Interestingly, more extensive bone bridging at the fracture site was observed in the LIPUS-treated femur (Figs. 10B and 10C) than in the control femur (Fig. 10A) in not only the T group but also in the Ph-3 group on day 25. Bone bridging by new bone formation had not occurred substantially in the LIPUS-untreated control femur (Fig. 10A). The LIPUS-treated femur in the Ph-3 group (Fig. 10B) on day 25 had received LIPUS treatment from day 17 to 24 (for 8 days), and that in the T group (Fig. 10C) on day 25, from day 1 to 24 (for 24 days) after the fracture. In the LIPUS-treated femur, the bridging of newly formed cortex and trabecular bone in the fracture callus was greater in the T group than in the Ph-3 group.

DISCUSSION

Fracture healing can be accelerated by exposure to LIPUS in both animal fracture models and clinical trials.[3–9] However, the underlying mechanism of action remains unclear. In this study, we investigated the effects of the duration and timing of LIPUS treatment on the benefits of LIPUS on the

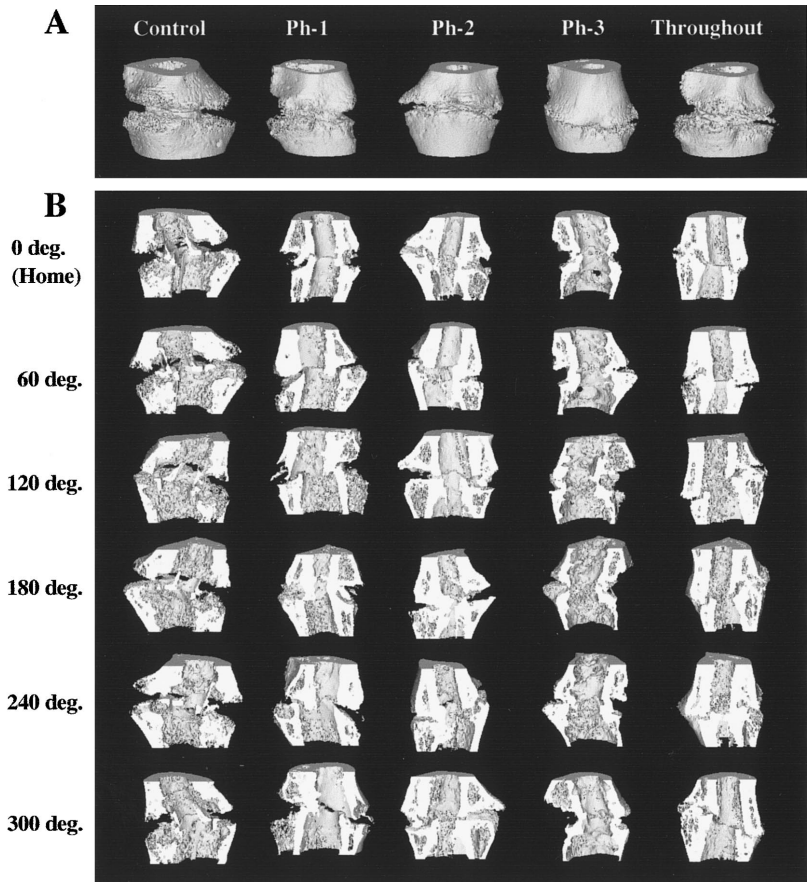

FIG. 4. 3D reconstructions from 100 μCT tomograms (each 80 μm in thickness) of fractured femora treated with LIPUS or nontreated on day 25 after the fracture. Reconstructions of nontreated femur in the T group and LIPUS-treated femurs in Ph-1, Ph-2, Ph-3, and T groups are shown.

healing of rat femoral fractures to find a target reaction of LIPUS in the fracture healing process.

Maximal torque of the LIPUS-treated side was significantly higher than that of the contralateral control side in all groups. These results show that partial LIPUS treatment is able to accelerate fracture healing regardless of its timing. Furthermore, maximal torque of the LIPUS-treated femur in the T group was significantly higher than that in the other three groups, probably because the accelerating effect of LIPUS was additive. These data also suggest that LIPUS acts on some kind of cellular reaction involved in the fracture healing process.

The mechanical properties (i.e., torsional torque and stiffness) of the fracture callus in long bones reflect the extent of fracture union as a result of healing in the fracture site.[22,23] In this study, maximal torque of the LIPUS-treated femur was significantly greater than that of the control side in all groups, but there was no significant difference between the LIPUS-treated side and the control side for BMC at the femoral fracture site or for the HCA in any of the groups. These findings indicate that the promoting effects of LIPUS on the mechanical properties of the fracture callus involve the fracture union but not the size and/or bone mass of the fracture callus on day 25 after the fracture.

The results for the multiple viewing of 3D μCT reconstructions at the fracture site were coincident with the data for mechanical testing. Although several investigators showed that the density and connectivity of bone in the fracture callus was important to increase the rigidity of the callus,[24–26] our observations in this study suggest that the efficiency of fracture union also contributes to the advanced mechanical properties of the fracture callus. Here, we describe for the first time that the multiple viewing from various angles (60° pitch) using 3D μCT reconstructions of the fracture callus is a powerful tool for estimation of the bone union and the fracture callus condition both visually and quantitatively.

In the histological analysis, endochondral ossification on day 9 and day 17, and the bone remodeling and bone bridging on day 17 and day 25 had advanced more in LIPUS-treated femurs than in the control femurs, respectively. These observations assured the results from the mechanical testing and multiple viewing by μCT. The partial LIPUS treatments (8-day treatment) only in Ph-1, Ph-2, or Ph-3 were effective in advancing endochondral ossification and/or bone remodeling in the fracture callus. These results suggest that LIPUS influenced some cellular reactions active at each time period. However, it is unclear which reaction is the target of LIPUS and how LIPUS affects it.

The micromechanical strains produced by LIPUS's pressure waves in living tissue can result in biochemical events at the cellular level. In accordance with this, it seems to be easy that a cell type that has a sensitivity to mechanical strains would respond to LIPUS. Although further investi-

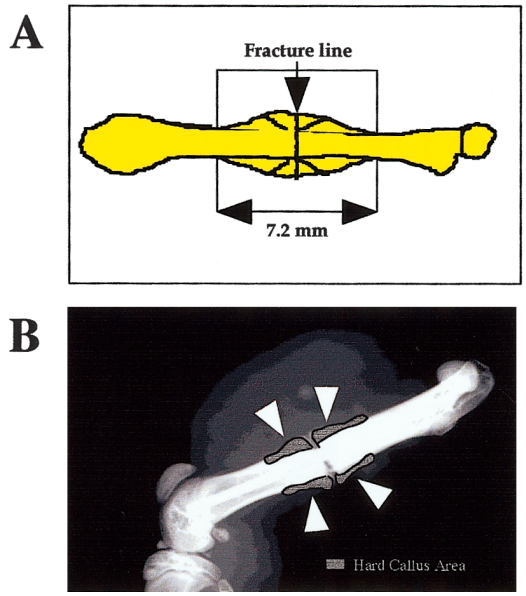

FIG. 5. (A) The BMC of femoral diaphysis at fracture site was measured, and (B) anterior and posterior HCAs were traced and measured with image analysis software.

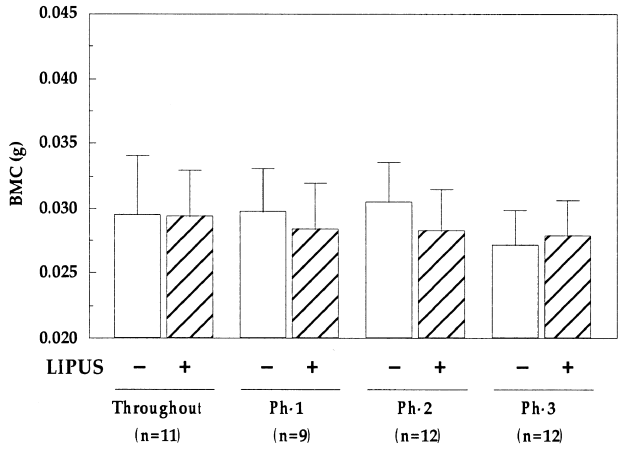

FIG. 7. Effects of LIPUS treatment of various durations and timings on BMC of the fracture callus near the fracture site on day 25 after the fracture. The HCA of the nontreated femur and LIPUS-treated femur is represented as open bars and closed bars, respectively. There was no significant difference in BMC between the nontreated femur and the LIPUS-treated femur in the T group ($n = 11$), Ph-1 group ($n = 9$), Ph-2 group ($n = 12$), or Ph-3 group ($n = 12$). The horizontal bars represent ± 1SD. Paired *t*-testing was used for statistical analysis.

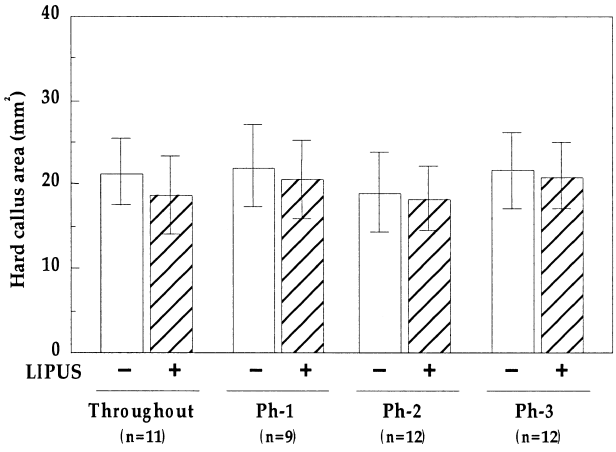

FIG. 6. Effects of LIPUS treatment of various durations and timings on the HCA of the fracture callus on day 25 after the femoral fracture. The HCA of nontreated femur or LIPUS-treated femur is represented as open bars or closed bars, respectively. There was no significant difference in the HCA between the nontreated femur and LIPUS-treated femur in the T group ($n = 11$), Ph-1 group ($n = 9$), Ph-2 group ($n = 12$), or Ph-3 group ($n = 12$). The horizontal bars represent ±1 SD. Paired *t*-testing was used for statistical analysis.

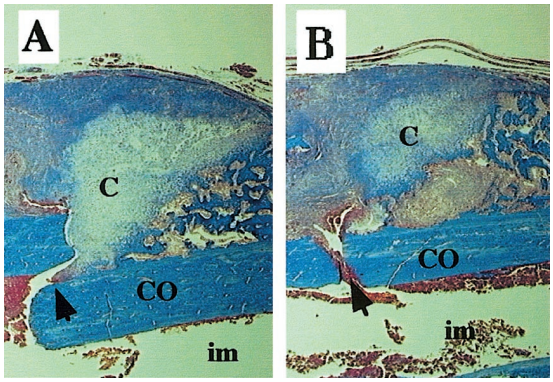

FIG. 8. Effects of LIPUS treatment on the histology of fracture healing at day 9. Photomicrographs show the appearance of the fracture healing in (A) the control limb and (B) the treated limb. Early endochondral ossification on day 9 in the LIPUS-treated femur was greater than in the control. Sections were stained with Masson's trichrome stain. Arrowheads show the fracture sites. Specific regions are labeled as follows: cortical bone, co; muscle, m; intramedullary canal, im; and cartilage, c.

gations are needed to define the target cells in each time period, the results obtained in the present study allow us to make the following speculation about the candidate:

(1) Inflammatory reaction. In the inflammatory phase, a hematoma is formed from blood vessels ruptured by the injury; and soon thereafter, inflammatory cells such as macrophages and/or lymphocytes invade the clot. It was reported that macrophages contain a stretch-sensitive potassium channel, the activity of which was modified by mechanical stress.[27,28] Furthermore, it was reported that high-energy ultrasound modulated the activity of thymocytes.[29]

(2) Blood flow and neovascularization. After or overlapping the end stage of inflammatory reactions, the formation of granulation tissue and the invasion of multipotential mesenchymal stem cells occur. In this stage, the concurrent proliferation of blood vessels within the periosteal tissues and marrow space helps to route the appropriate cells to the fracture site. Rawool et al.

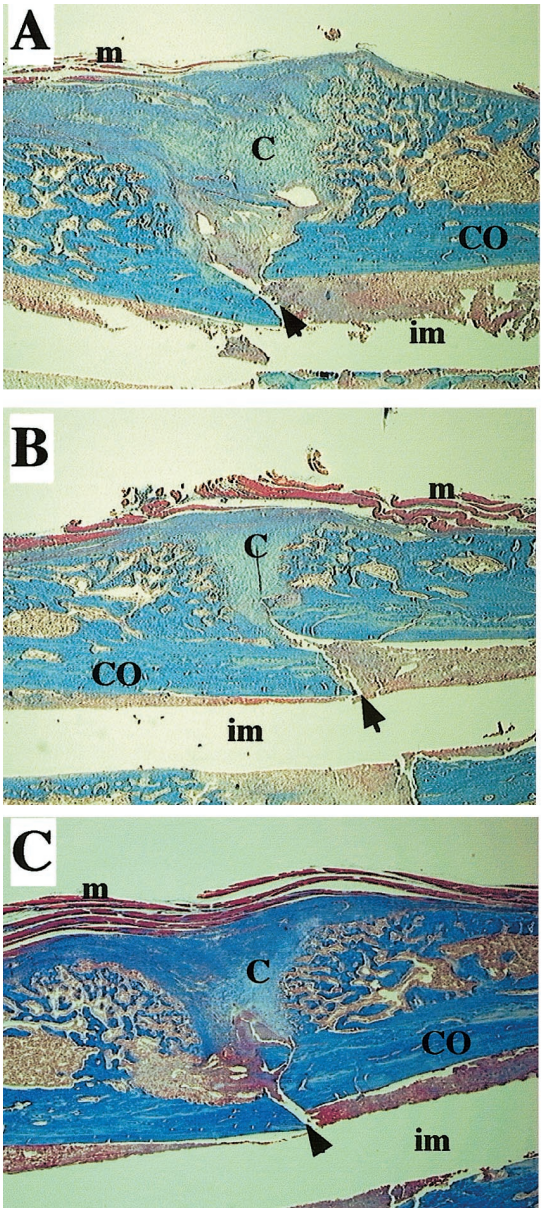

FIG. 9. This shows the effect of 8 days of treatment versus 16 days of treatment. On day 17, endochondral ossification and early remodeling were less in the (A) control femur than in the (B) 16 days of LIPUS-treated femur or (C) 8 days of LIPUS-treated femur. The size of the mature cartilage in the LIPUS-treated femur was smaller and the number of osteoclasts was more in the LIPUS-treated femora than in the control.

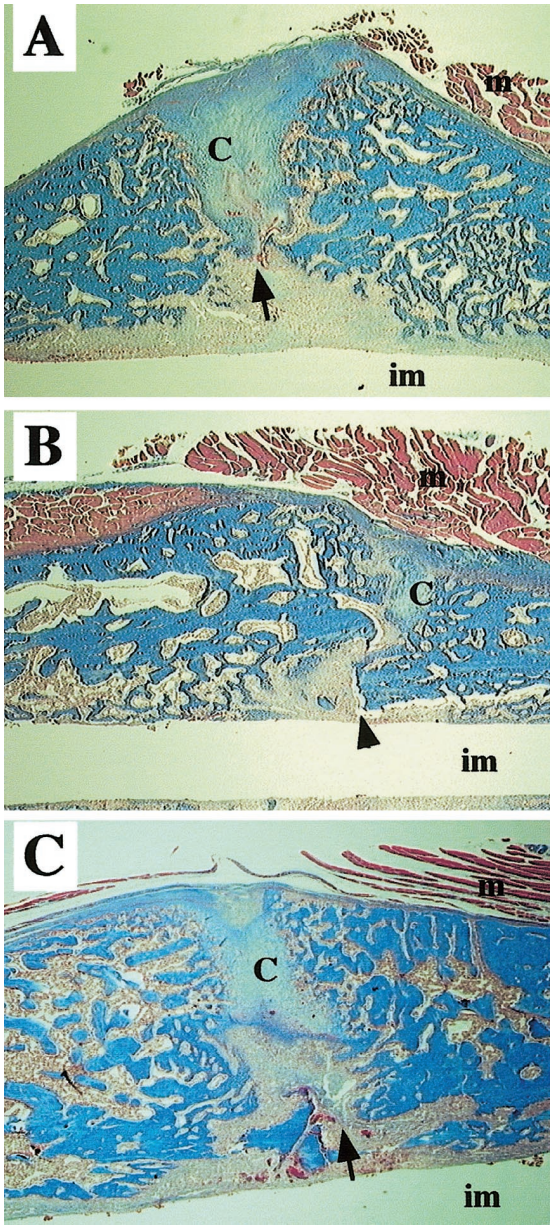

FIG. 10. On day 25, (A) the control femur had less extensive bone bridging than the femur treated for (B) 24 days or (C) 8 days. The bridging of newly formed cortex and trabecular bone in the fracture callus was greater in panel B than in panel C.

showed that LIPUS increased the degree of vascularity in an osteomized dog ulna model of fracture healing.[30] This effect was observed from 1 to 3 days after the fracture to over 10 days thereafter, and we showed that LIPUS stimulated platelet-derived growth factor (PDGF) production in the coculture human endothelial cells with human osteoblasts in vitro.[31]

(3) Intramembranous ossification. Periosteum-derived cells, which are of the osteoblastic lineage, may be involved in intramembranous ossification.[32] Ryaby et al. reported that LIPUS increased calcium incorporation in differentiating cartilage and bone cell cultures.[33,34] This increased second messenger activity was paralleled by the modulation of adenylate cyclase activity and transforming growth factor β (TGF-β) synthesis in osteoblastic cells.[34] Furthermore, other investigators reported that topical application of TGF-β to long bones stimulated osteogenesis in the periosteum.[35–37]

(4) Chondrogenesis. Parvizi et al. reported that ultrasound modulated second messenger activity in primary rat chondrocytes.[38] They showed that application of ul-

trasound at 50 mW/cm^2 and at higher intensities induced a real-time increase in the intracellular level of calcium. And other investigators showed that exposure of cultured chondrocytes to LIPUS stimulated an up-regulation of aggrecan gene expression.[39,40]

(5) Endochondral ossification. Invasion of newly formed blood vessels into the cartilage tissue, degradation of cartilage tissue, and bone formation are involved in endochondral ossification. The growth, differentiation and activity of the cells such as chondrocytes, osteoblasts, endothelial cells, and chondroclasts/osteoclasts related to those reactions may be important in this process. In a previous study, we showed that the number of multinuclear cells (MNCs) near the boundary between cartilage tissue and trabecular bone in the LIPUS-treated femur (15 $\pm$ 3 MNCs/mm) was greater in comparison with that in the control femur (8 $\pm$ 2 MNCs/mm) on day 21 after the fracture (in preparation). However, it is unclear whether this effect was based on the direct action of LIPUS on osteoclastogenesis. Soma et al. showed that the application of bilateral stretch stress to osteoblastic cells stimulated the production of some factors that could up-regulate osteoclastogenesis.[41]

(6) Bone remodeling. Tanzer et al. reported that LIPUS stimulated bone ingrowth into porous coated dog femoral implants.[42] In contrast, Spadaro et al. reported that physeal bone growth was far less sensitive to LIPUS than was fracture repair.[43] It remains unclear whether and/or how LIPUS directly modulates bone metabolism involved in bone formation and bone resorption.

In conclusion, we investigated whether the accelerating effects of LIPUS on the healing of rat femoral fractures depended on the duration and timing of LIPUS treatment to determine the target reaction of LIPUS in the fracture healing process. Although we could not define the main target, we found out that LIPUS accelerated the rat femoral fracture healing regardless of the timing of LIPUS treatment. Thus, LIPUS appears to act on various cellular reactions involved in the fracture healing process.

REFERENCES

1. Ziskin MC 1987 Application of ultrasound in medicine—comparison with other modalities. In: Rapacholi MH, Grandolfo M, Rindi A (eds.) Ultrasound: Medical Applications, Biological Effects, and Hazard Potential. Plenum Press, New York, NY, USA, pp. 49–59.
2. Wells PNT 1985 Surgical applications of ultrasound. In: Nyborg WL, Ziskin MC (eds.) Biological Effects of Ultrasound. Churchill Livingstone, New York, NY, USA, pp. 157–167.
3. Xavier CAM, Duarte LR 1983 Estimulaci ultra-sonica de callo osseo: Applicaca clinica. Rev Bras Orthop **18:**73–80.
4. Duarte LR 1983 The stimulation of bone growth by ultrasound. Arch Orthop Trauma Surg **101:**153–159.
5. Klug W, Franke WG, Knoch HG 1986 Scintigraphic control of bone-fracture healing under ultrasonic stimulation: An animal experimental study. Eur J Nucl Med **11:**494–497.
6. Pilla AA, Mont MA, Nasser PR, Khan SA, Figueiredo M, Kaufman JJ, Siffert RS 1990 Non-invasive low-intensity pulsed ultrasound accelerates bone healing in the rabbit. J Orthop Trauma **4:**246–253.
7. Wang S-J, Lewallen DG, Bolander ME, Chao EYS, Ilstrup DM, Greenleaf JF 1994 Low intensity ultrasound treatment increases strength in a rat femoral fracture model. J Orthop Res **12:**40–47.
8. Heckman JD, Ryaby JP, McCabe J, Frey JJ, Kilcoyne RF 1994 Acceleration of tibial fracture-healing by non-invasive, low-intensity pulsed ultrasound. J Bone Joint Surg Am **76:**26–34.
9. Kristiansen TK, Ryaby JP, McCabe J, Frey JJ, Roe LR 1997 Accelerated healing of distal radial fractures with the use of specific, low-intensity ultrasound. A multicenter, prospective, randomized, double-blind, placebo-controlled study. J Bone Joint Surg Am **79:**961–973.
10. Binderman I, Zor U, Kaye AM, Shimshoni Z, Harell A, Somjen D 1988 The transduction of mechanical force into biochemical events in bone cells may involve activation of phospholipase A_2. Calcif Tissue Int **42:**261–266.
11. Buckley MJ, Banes AJ, Levin LG, Sumpio BE, Sato M, Jordan R, Gilbert J, Link GW, Tran Son Tay R 1988 Osteoblasts increase their rate of division and align in response to cyclic, mechanical tension in vitro. Bone Miner **4:**225–236.
12. Rubin J, Biskobing D, Fan X, Rubin C, McLeod K, Taylor WR 1997 Pressure regulates osteoclast formation and MCSF expression in marrow culture. J Cell Physiol **170:**81–87.
13. Bolander ME 1992 Regulation of fracture repair by growth factors. Proc Soc Exp Biol Med **200:**165–170.
14. Schwachtgen JL, Houston P, Campbell C, Sukhatme V, Braddock M 1998 Fluid shear stress activation of egr-1 transcription in cultured human endothelial and epithelial cells is mediated via the extracellular signal-related kinase 1/2 mitogen-activated protein kinase pathway. J Clin Invest **101:**2540–2549.
15. MacKenna DA, Dolfi F, Vuori K, Ruoslahti E 1998 Extracellular signal-regulated kinase and c-Jun NH2-terminal kinase activation by mechanical stretch is integrin-dependent and matrix-specific in rat cardiac fibroblasts. J Clin Invest **101:**301–310.
16. Pavalko FM, Chen NX, Turner CH, Burr DB, Atkinson S, Hsieh YF, Qiu J, Duncan RL 1998 Fluid shear-induced mechanical signaling in MC3T3–E1 osteoblasts requires cytoskeleton-integrin interactions. Am J Physiol **275:**C1591–C1601.
17. Quinn TM, Grodzinsky AJ, Buschmann MD, Kim YJ, Hunziker EB 1998 Mechanical compression alters proteoglycan deposition and matrix deformation around individual cells in cartilage explants. J Cell Sci **111:**573–583.
18. Ajubi NE, Klein-Nulend J, Alblas MJ, Burger EH, Nijweide PJ 1999 Signal transduction pathways involved in fluid flow-induced PGE2 production by cultured osteocytes. Am J Physiol **276:**E171–E178.
19. Einhorn TA 1998 The cell and molecular biology of fracture healing. Clin Orthop **55**(Suppl 3)**:**S7–S21.
20. Jingushi S, Joyce ME, Bolander ME 1992 Genetic expression of extracellular matrix proteins correlates with histologic changes during fracture repair. J Bone Miner Res **7:**1045–1055.
21. Bonnarens F, Einhorn TA 1984 Production of a standard closed fracture in laboratory animal bone. J Orthop Res **2:**97–101.
22. White AA III, Panjabi MM, Southwick WO 1977 The four biomechanical stages of fracture repair. J Bone Joint Surg Am **59:**188–192.
23. Black J, Perdigon P, Brown N, Pollack SR 1984 Stiffness and strength of fracture callus. Relative rates of mechanical maturation as evaluated by a uniaxial tensile test. Clin Orthop **182:**278–288.
24. Markel MD, Wikenheiser MA, Chao EY 1990 A study of fracture callus material properties: Relationship to the torsional strength of bone. J Orthop Res **8:**843–850.

25. Chakkalakal DA, Lippiello L, Wilson RF, Shindell R, Connolly JF 1990 Mineral and matrix contributions to rigidity in fracture healing. J Biomech **23:**425–434.
26. Augat P, Merk J, Genant HK, Claes L 1997 Quantitative assessment of experimental fracture repair by peripheral computed tomography. Calcif Tissue Int **60:**194–199.
27. Martin DK, Bootcov MR, Campbell TJ, French PW, Breit SN 1995 Human macrophages contain a stretch-sensitive potassium channel that is activated by adherence and cytokines. J Membr Biol **147:**305–315.
28. Mattana J, Sankaran RT, Singhal PC 1995 Repetitive mechanical strain suppresses macrophage uptake of immunoglobulin G complexes and enhances cyclic adenosine monophosphate synthesis. Am J Pathol **147:**529–540.
29. Dooley DA, Child SZ, Carstensen EL, Miller MW 1983 The effects of continuous wave and pulsed ultrasound on rat thymocytes in vitro. Ultrasound Med Biol **9:**379–384.
30. Rawool NM, Goldberg BB, Forsberg F, Winder AA, Tallah RJ, Hume E 1997 Power doppler assessment of vascular changes during fracture treatment with low intensity ultrasound. Trans 83rd Radiol Soc North Am **83:**421.
31. Ito M, Azuma Y, Ohta T, Komoriya K 2000 Effects of ultrasound and 1,25-dihydroxyvitamin D3 on growth factor secretion in co-cultures of osteoblasts and endothelial cells. Ultrasound Med Biol **26:**161–166.
32. Utvag SE, Grundnes O, Reikeras O 1999 Early muscle-periosteal lesion inhibits fracture healing in rats. Acta Orthop Scand **70:**62–66.
33. Ryaby JT, Bachner EJ, Bendo JA, Dalton PF, Tannenbaum S, Pilla AA 1989 Low intensity pulsed ultrasound increases calcium incorporation in both differentiating cartilage and bone cell cultures. Trans Orthop Res Soc **14:**15.
34. Ryaby JT, Mathew J, Duarte-Alves P 1992 Low intensity pulsed ultrasound affects adenylate cyclase and TGF-β synthesis in osteoblastic cells. Trans Orthop Res Soc **17:**590.
35. Joyce ME, Roberts AB, Sporn MB, Bolander ME 1990 Transforming growth factor-beta and the initiation of chondrogenesis and osteogenesis in the rat femur. J Cell Biol **110:**2195–2207.
36. Joyce ME, Jingushi S, and Bolander ME 1990 Transforming growth factor-beta in the regulation of fracture repair. Orthop Clin North Am **21:**199–209.
37. Taniguchi Y, Tanaka T, Gotoh K, Satoh R, Inazu M 1993 Transforming growth factor beta-1 induced cellular heterogeneity in the periosteum of rat parietal bones. Calcif Tissue Int **53:**122–126.
38. Parvizi J, Parpura V, Kinnick RR, Greenleaf JF, Bolander ME 1997 Low intensity ultrasound increases intracellular concentration of calcium in chondrocytes. Trans Orthop Res Soc **22:**465.
39. Yang K-H, Parvizi J, Wang S-J, Lewallen DG, Kinnick RR, Greenleaf JF, Bolander ME 1996 Exposure to low-intensity ultrasound increases aggrecan gene expression in a rat femur fracture model. J Orthop Res **14:**802–809.
40. Wu C-C, Lewallen DG, Bolander ME, Bronk J, Kinnick R, Greenleaf JF 1996 Exposure to low intensity ultrasound stimulates aggrecan gene expression by cultured chondrocytes. Trans Orthop Res Soc **21:**622.
41. Soma S, Matsumoto S, Takano-Yamamoto T 1997 Enhancement by conditioned medium of stretched calvarial bone cells of the osteoclast-like cell formation induced by parathyroid hormone in mouse bone marrow cultures. Arch Oral Biol **42:**205–211.
42. Tanzer M, Harvey E, Kay A, Morton P, Bobyn JD 1996 Effect of noninvasive low intensity ultrasound on bone growth into porous-coated implants. J Orthop Res **14:**901–906.
43. Spadaro JA, Albanese SA 1998 Application of low-intensity ultrasound to growing bone in rats. Ultrasound Med Biol **24:**567–573.

Address reprint requests to:
Yoshiaki Azuma, Ph.D.
Pharmacological Research Department
Teijin Institute for Biomedical Research, Teijin Limited
4–3-2 Asahigaoka, Hino City
Tokyo 191-8512, Japan

Received in original form July 30, 1999; in revised form October 31, 2000; accepted October 31, 2000.